

LINC01123 acts as an oncogenic driver in lung adenocarcinoma by regulating the miR-4766-5p/PYCR1 axis

Hong Wang* and Dongsheng He*

Department of Cardiothoracic Surgery, The First Affiliated Hospital of Chengdu Medical College, Chengdu, Sichuan, China

*These authors equally contributed to this work

Summary. Background. Lung adenocarcinoma remains one of the most significant threats to human life as it involves multiple etiologies, including alteration of oncogenes or tumor-inhibitory genes. Long non-coding RNAs (lncRNAs) have been reported to have both cancer promoting and cancer inhibiting effects. In this work, we investigated the function and mechanism of lncRNA LINC01123 in lung adenocarcinoma.

Methods. The expression of LINC01123, miR-4766-5p, and PYCR1 (pyrroline-5-carboxylate reductase 1) mRNA was analyzed by RT-qPCR. The protein expression levels of PYCR1 and the apoptosis-related proteins (Bax and Bcl-2) were determined by western blotting. Cell proliferation and migration were determined by CCK-8 and wound-healing assays, respectively. Tumor growth in nude mice and Ki67 immunohistochemical staining were used to determine the *in vivo* role of LINC01123. The putative binding relationships miR-4766-5p has with LINC01123 and PYCR1, which had been identified by analysis of public databases, were validated through RIP and dual-luciferase reporter assays.

Results. LINC01123 and PYCR1 overexpression and miR-4766-5p downregulation were shown to occur in lung adenocarcinoma samples. LINC01123 depletion repressed lung adenocarcinoma cell growth and migration and blocked the development of solid tumors in an animal model. Moreover, LINC01123 bound directly to miR-4766-5p, the downregulation of which attenuated the anticancer effects of LINC01123 depletion in lung adenocarcinoma cells. MiR-4766-5p directly targeted downstream PYCR1 to suppress PYCR1 expression. The repressive effects of PYCR1 knockdown on the migration and proliferation of lung

adenocarcinoma cells were also partly abolished by miR-4766-5p downregulation.

Conclusion. Downregulation of LINC01123 represses lung adenocarcinoma progression. This suggests that LINC01123 functions as an oncogenic driver in lung adenocarcinoma by controlling the miR-4766-5p/PYCR1 axis.

Key words: LINC01123, Lung adenocarcinoma, miR-4766-5p, PYCR1

Introduction

Lung cancer is one of the most commonly diagnosed malignant tumors, with its incidence being second only to breast cancer according to the 2020 Global Cancer Data (Sung et al., 2021). Although overall survival rates for lung cancer have improved in recent years, they remain unsatisfactory (<21%) (Lu et al., 2019). As the most prevalent type of lung cancer, lung adenocarcinoma accounts for approximately 50% of all lung cancer cases (Siegel et al., 2017). The molecular mechanism of lung adenocarcinoma involves activation and inactivation of multiple oncogenic or cancer-inhibiting factors, such as functional genes and non-coding RNAs (Stella et al., 2013; Tutar et al., 2016). Nonetheless, the complex progression of carcinogenesis and insufficient screening regimens result in advanced or metastatic lung adenocarcinoma when patients are diagnosed with lung adenocarcinoma (Gridelli et al., 2015). There is, therefore, a clear need for in-depth exploration of factors involved in the oncogenic process to improve the diagnosis and therapy of lung adenocarcinoma.

Long non-coding RNAs (lncRNAs) have sequences that are more than two hundred nucleotides in length. Several reports have shown that lncRNAs participate in a variety of essential biological processes, such as human aging, systemic diseases, and alteration of the

Corresponding Author: Dr. Hong Wang, Department of Cardiothoracic Surgery, The First Affiliated Hospital of Chengdu Medical College, No. 278, Middle Section of Baoguang Avenue, Xindu District, Chengdu 610500, Sichuan, China. e-mail: hongwang59@163.com
www.hh.um.es. DOI: 10.14670/HH-18-610



tumor microenvironment (Gomez-Verjan et al., 2018; Lee et al., 2020; Shi et al., 2021). LncRNAs have multiple effects on cancer cell growth and mobility, immune responses, drug resistance, and energy metabolism (Martens-Uzunova et al., 2014; Zamaraev et al., 2021). In light of this, lncRNAs have become established diagnostic markers and therapeutic targets for a variety of malignant carcinomas (Martens-Uzunova et al., 2014; Zamaraev et al., 2021). By interacting with nucleic acids and proteins, lncRNAs can act as enhancers, scaffolds, or decoys for a variety of carcinogens and tumor suppressors (Zamaraev et al., 2021). Numerous lncRNAs have been functionally expounded in lung cancer. For instance, LINC00336 has been overexpressed in lung cancer, which resulted in inhibition of ferroptosis and thus stimulation of the growth of lung cancer cells (Wang et al., 2019b). Upregulation of LINC01123 in lung adenocarcinoma was discovered in the public GEPIA database (<http://gepia.cancer-pku.cn/detail.php?gene=LINC01123>). Moreover, LINC01123 decoyed miR-199a-5p to enhance the expression of oncogenic c-Myc, thus reinforcing aerobic glycolysis and the proliferation of lung cancer cells (Hua et al., 2019). The carcinogenic effects of LINC01123 have been partially established in lung cancer. However, the functional effects of LINC01123 in lung adenocarcinoma have yet to be fully elucidated. Additionally, its potential functional mechanisms require further exploration.

MiR-4766-5p has been documented to result in tumor-repressive effects in numerous cancers, including breast cancer and gastric cancer (Liang et al., 2018; Wei et al., 2019). Nevertheless, the potency of miR-4766-5p in lung adenocarcinoma development is not clear. Interestingly, miR-4766-5p has been predicted to contain binding sites for LINC01123. Hence, we explored whether LINC01123 had sponge-like effects on miR-4766-5p in lung cancer development. It is widely known that miRNAs combine with the 3'-UTR of target genes to alter gene expression (Lee and Vasudevan, 2013). In this regard, the targets of miR-4766-5p, such as sirtuin 1 (SIRT1) and NF- κ B-activating protein (NKAP), have been shown to be involved in miR-4766-5p-mediated carcinogenesis (Liang et al., 2018; Wei et al., 2019). There are still numerous functional genes potentially targeted by miR-4766-5p that have yet to be identified, such as pyrroline-5-carboxylate reductase 1 (PYCR1). PYCR1 has been reported to be overexpressed in lung cancer samples, and PYCR1 silencing restrains multiple malignant phenotypes in lung cancer cells (Cai et al., 2018; Gao et al., 2020). However, the interplay between PYCR1 and miR-4766-5p in lung adenocarcinoma progression has yet to be investigated.

In this study, we mainly explored the partial functions of LINC01123 and confirmed its underlying molecular association with the miR-4766-5p/PYCR1 axis. To our knowledge, we are the first to report the binding between miR-4766-5p and LINC01123 or PYCR1. We also investigated the role of their interactions in lung adenocarcinoma development, with

the aim of gaining new molecular insights regarding the function of LINC01123 in lung adenocarcinoma.

Materials and methods

Tissue specimens

Patients who were first diagnosed with primary lung adenocarcinoma and underwent surgical operation at the First Affiliated Hospital of Chengdu Medical College were enrolled in our study. Patients who failed to provide written informed consent, received any previous chemotherapy or radiotherapy for cancer treatment, or had other malignant cancers or systemic diseases were excluded. There were 38 pairs of tumor samples and normal samples in our study. The frozen tissues were stored in -80°C freezers. The design and implementation of this project were approved by the Ethics Committee of The First Affiliated Hospital of Chengdu Medical College. The clinicopathological characteristics of the 38 patients with lung adenocarcinoma are listed in Table 1.

Cell lines

The non-cancer control cell line BEAS-2B and the lung adenocarcinoma cell lines A549, Calu-3, and PC9 were purchased from BeNa (Beijing, China). The DV-90 lung adenocarcinoma cell line was obtained from QianNuo Biotechnology (Hangzhou, China). BEAS-2B, Calu-3, PC9, and DV-90 cells were cultivated in DMEM (BeNa) containing 10% FBS (BeNa). A549 cells were cultured in RPMI1640 medium (BeNa) containing 10% FBS. The cultures were maintained in incubators at 37°C in a 5% CO_2 atmosphere.

RT-qPCR

Total RNA was isolated using TRIzol[®] reagent (Solarbio, Beijing, China) following the supplied

Table 1. The clinicopathological characteristics of 38 patients with lung adenocarcinoma.

Clinicopathological characteristics	Cases (n=38)
Age	
≥ 58	19
< 58	19
Gender	
Male	21
Female	17
Tumor size, diameter (cm)	
≥ 3.5	16
< 3.5	22
TNM stage	
I-II	20
III-IV	18
Tumor differentiation	
Well	18
Moderate	13
Poor	7

LINC01123 drives lung adenocarcinoma progression

protocol. With the aid of an miRNA 1st Strand Synthesis Kit (Cwbio, Beijing, China) and a HiScript[®] III 1st Strand cDNA Synthesis Kit (Vazyme, Nanjing, China), cDNAs were synthesized from 1 µg of total RNAs via reverse transcription. To analyze the expression, cDNA was supplemented with the UltraSYBR[™] Mixture (Cwbio) in a QuantStudio[™] System (Thermo Fisher Scientific, Waltham, USA), using U6 or GAPDH as the internal references. The PCR conditions were as follows: 95°C for 10 min (1 cycle), 95°C for 10 s, and 60°C for 1 min (40 cycles). The Ct values were processed by applying the 2^{-ΔΔCt} method. The primer sequences are listed in Table 2.

Subcellular localization

Total RNAs were isolated from the cytoplasmic and nuclear fractions of Calu-3 and A549 cells using a PARIS[™] kit (Thermo Fisher Scientific), following the product protocol. GAPDH was used as the reference for the cytoplasm while U6 was used as a nuclear marker. The abundance of LINC01123 in the separated fractions was determined by RT-qPCR.

Cell transfection

For LINC01123 knockdown, small interfering RNA (siRNA) targeting LINC01123 (si-lnc) or PYCR1 (si-PYCR1) and the scrambled sequence negative control (si-NC) were obtained from GenePharma (Shanghai, China). MiR-4766-5p mimic, miR-4766-5p inhibitor, mimic-NC, and inhibitor-NC were all purchased from RiboBio (Guangzhou, China). These oligonucleotides were individually or simultaneously transfected into A549 and Calu-3 cells with the aid of a Lipofectamine[™] 3000 (Invitrogen, Carlsbad, USA). The efficiency of transfection was checked 24h post-transfection by western blotting or RT-qPCR analysis.

CCK-8 assay

The treated cells were seeded in 96-well plates at a density of 5×10³ cells per well and cultured at 37°C.

Table 2. Real-time PCR Primer synthesis list.

Gene	Sequences
LINC01123	Forward 5'-GTGCTTGAACGGCAGTAGC-3'
	Reverse 5'-AAGTGCACGGTGTGATAGGG-3'
miR-4766-5p	Forward 5'-GCCGAGTCTGAAAGAGCAGTT-3'
	Reverse 5'-CAGTGCAGGGTCCGAGGTAT-3'
PYCR1	Forward 5'-TGAAGCCACACATCATCCCC-3'
	Reverse 5'-CCCATCTTCACACCCCATC-3'
U6	Forward 5'-CTCGCTTCGGCAGCAC-3'
	Reverse 5'-AACGCTTCACGAATTTGCGT-3'
GAPDH	Forward 5'-AGAAAAACCTGCCAAATATGATGAC-3'
	Reverse 5'-TGGGTGTCGCTGTTGAAGTC-3'

After 0, 24, 48, and 72h of incubation, the cells were treated with CCK-8 reagent (Solarbio) for an additional two hours. After treatment, the absorbance of the wells at 450 nm was determined using a microplate reader (Thermo Fisher Scientific).

Wound-healing assay

The treated lung adenocarcinoma cells were seeded in 24-well plates (5×10³ cells) and cultured overnight to reach 80% confluence. A 200 µL sterile pipette tip was used to scratch the cell surface. The dissociated cells were rinsed with PBS, followed by the addition of 2 mL of serum-free medium. The wound distance was imaged with a microscope (Nikon, Tokyo, Japan). After incubating the cells for 24h, the wound distance was imaged again.

Western blotting

RIPA reagent (Solarbio) and a BCA Protein Assay Kit (Solarbio) were utilized to extract and quantify total proteins. The proteins (20 µg/lane) were separated by 10% SDS-PAGE and then transferred to PVDF membranes. The membranes were incubated in 5% skim milk for blocking (room temperature, 2h) followed by incubation with primary antibodies (4°C, overnight) and a secondary antibody (room temperature, 2h), all of which were obtained from Abcam (Cambridge, USA). Details regarding the antibodies are as follows: anti-Bax (ab32503; 1/2000), anti-Bcl-2 (ab32124; 1/1000), anti-PYCR1 (ab102601; 1/1000), anti-GAPDH (ab9485; 1/2500), and goat anti-rabbit IgG (ab205718; 1/5000). The protein signals were detected using an ECL Kit (Solarbio).

Tumor growth in nude mice

Short hairpin RNAs (shRNAs) that target LINC01123 (sh-lnc), as well as sh-NC, were designed, synthesized, and then packaged into lentiviruses by Genepharma. The experimental nude mice (female, 6-week-old) were provided by Vital River (Beijing, China) and acclimated to room conditions for a week. A549 cells (2×10⁶ cells/mouse) were infected with lentivirus sh-lnc (n=5) for stable LINC01123 knockdown or with sh-NC (n=5). The cells were then injected subcutaneously into the nude mice. Throughout the period of tumor development, the tumor volume (length×width²×0.5) was evaluated once a week. Finally, after 5 weeks, the tumors were excised following the euthanasia of the mice. The animal procedures were approved by the First Affiliated Hospital of Chengdu Medical College.

Immunohistochemistry (IHC) staining for Ki67

The tumor tissues from nude mice were embedded in paraffin and cut into 4 µm sections for IHC staining. The

LINC01123 drives lung adenocarcinoma progression

paraffin-embedded sections were then dewaxed with xylene, hydrated with a gradient of ethanol, and treated with 3% H₂O₂/methanol solution for 30 min. The sections were then treated with sodium citrate solution for 15 min, blocked with 3% BSA/PBS solution for 1h, and incubated with a Ki67 antibody (Cat# ab15580, Abcam, USA) overnight at 4°C. The next day, the sections were incubated with secondary antibody (Cat# ab7090, Abcam, USA) for 1h. A DAB Horseradish Peroxidase Color Development Kit (Beyotime, China) was then used to visualize the target immunoreactive complex. The Ki67-positive cells were observed at 200× magnification.

Dual-luciferase reporter assay

The public databases StarBase and TargetScan were employed to identify LINC01123 and miR-4766-5p targets. Their potential binding sites were confirmed by dual-luciferase reporter assays. In brief, the partial sequences of the PYCR1 3'-UTR and LINC01123 that had miR-4766-5p binding sites were assembled and cloned into pmirGLO vectors (Promega, Madison, USA) to generate wild-type (WT) LINC01123 and PYCR1 constructs. Additionally, the partial sequences of the PYCR1 3'-UTR and LINC01123 that had miR-4766-5p binding sites were assembled and inserted into the pmirGLO vectors to generate the mutant (MUT) constructs of LINC01123 and PYCR1. Each WT or MUT construct of LINC01123 and PYCR1 was then transfected along with mimic-NC or miR-4766-5p mimic into the experimental cells. Luciferase activity was assayed at 48h post-transfection by using a Dual-Luciferase Reporter Assay System (Promega).

RIP experiment

RIP was conducted using a Magna RIP™ Kit (Millipore, Bedford, USA) to investigate whether LINC01123 was involved in miR-4766-5p-mediated RISC. The experimental cells were lysed and then exposed to magnetic beads coated with anti-Ago2 or anti-IgG (control). RNA complexes enriched in Ago2 were captured by the beads and subsequently eluted using the TRIzol® reagent. Finally, miR-4766-5p and

LINC01123 enrichment was confirmed by RT-qPCR.

Statistical analysis

The data processing was performed with the statistical software GraphPad Prism 7.0 (GraphPad Prism, La Jolla, USA). The Shapiro-Wilk test was used to identify the distribution of variables, and all the data were parametric. The statistical analysis of the variations between or among groups was accomplished using Student's t-test or analysis of variance. The expression correlation between two groups was analyzed by Pearson's correlation analysis. All experiments were performed in triplicates, and the values are presented as the means±the standard deviation (SD). A $P < 0.05$ signified statistical significance.

Results

Elevated LINC01123 expression in lung adenocarcinoma

We first confirmed the expression and location of LINC01123 within the cells and tissue samples. Figure 1A shows that the levels of LINC01123 observed in the tumor specimens were higher compared to those of the normal samples. As expected, LINC01123 expression was also greatly elevated in A549, DV-90, Calu-3, and PC9 cells, unlike in BEAS-2B cells (Fig. 1B). A549 and Calu-3 cells were selected for the subsequent experiments due to the higher expression of LINC01123 in these two cell lines than in other lung adenocarcinoma cell lines. Cytoplasmic and nuclear RNAs were isolated from A549 and Calu-3 cells, and LINC01123 was found to be localized mainly in the cytoplasm (Fig. 1C). These data confirm the aberrantly high expression of LINC01123 in lung adenocarcinoma cells and tissues.

LINC01123 depletion restrained lung adenocarcinoma cell malignant behaviors and in vivo tumor development

To determine the function of LINC01123, it was knocked down in Calu-3 and A549 cells through their transfection with si-lnc (Fig. 2A). The cell proliferative potency of the si-lnc-transfected Calu-3 and A549 cells was greatly impaired compared to that of the si-NC-

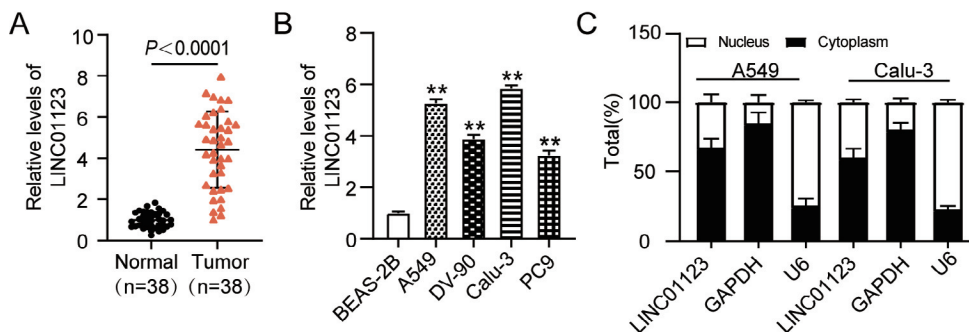


Fig. 1. High expression of LINC01123 was shown in lung adenocarcinoma. **A.** LINC01123 expression in lung adenocarcinoma tumor samples and normal samples. **B.** LINC01123 expression in non-cancer cell line (BEAS-2B) and lung adenocarcinoma cell lines (A549, DV-90, Calu-3 and PC9), ** $P < 0.01$ versus BEAS-2B. **C.** The location of LINC01123 in cytoplasmic and nuclear fraction of A549 and Calu-3 cells.

LINC01123 drives lung adenocarcinoma progression

transfected cells (Fig. 2B). Similarly, the migratory ability of si-lnc-transfected A549 and Calu-3 cells was considerably repressed, unlike that of those with si-NC (Fig. 2C). Moreover, we noticed that Bax levels were greatly increased, while Bcl-2 levels were considerably lower in A549 and Calu-3 cells transfected with si-lnc (Fig. 2D). This suggests that LINC01123 depletion resulted in cell apoptosis. In animal models, we observed that A549 cells with stable LINC01123 knockdown resulted in growth-restricted tumors, manifesting as smaller tumor volumes, weights, and sizes (Fig. 3A-C). Moreover, the Ki67 IHC staining assay revealed that the number of Ki67-positive cells was reduced in sh-lnc

group, suggesting that LINC01123 knockdown inhibited the tumor growth in vivo (Fig. 3D). Our data provide evidence that LINC01123 depletion represses lung adenocarcinoma progression.

LINC01123 bound to miR-4766-5p, which had an expression pattern opposite to that of LINC01123 in lung adenocarcinoma

StarBase was employed to computationally predict the miRNAs targeted by LINC01123. The resulting prediction revealed that miR-4766 and LINC01123 shared complementary sequences (Fig. 4A). To

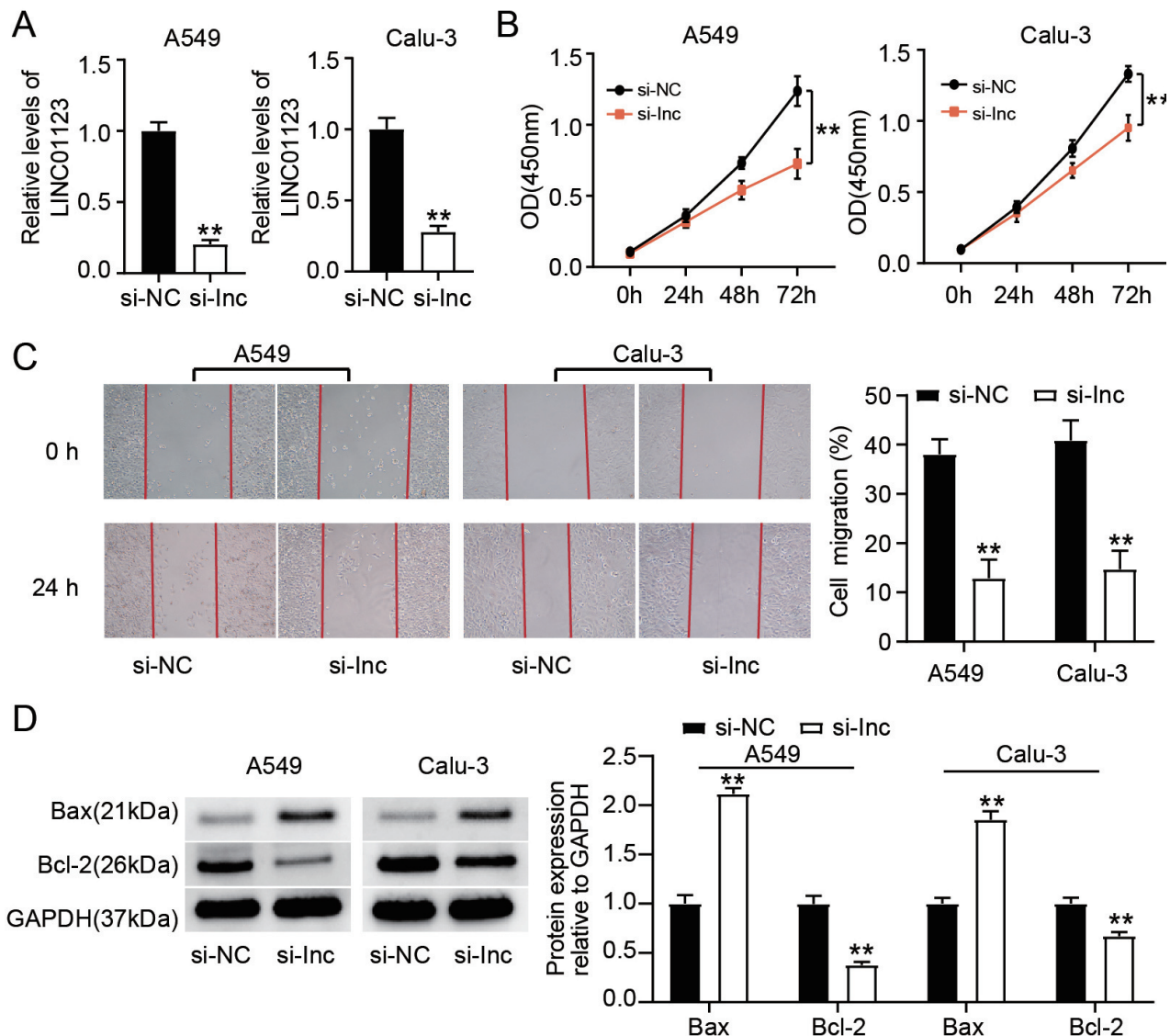


Fig. 2. LINC01123 depletion restrained lung adenocarcinoma progression. **A.** Si-lnc inhibitory efficiency in Calu-3 and A549 cells as ensured through RT-qPCR. **B.** The function of LINC01123 depletion on cell proliferation was examined by CCK-8 assay. **C.** The function of LINC01123 downregulation on cell migration was examined by wound-healing assay. **D.** The protein levels of Bax and Bcl-2 in cells after LINC01123 knockdown were checked by western blotting. ** $P < 0.01$ versus si-NC.

LINC01123 drives lung adenocarcinoma progression

substantiate the putative binding sites in their sequences, the WT and MUT constructs of LINC01123 were assembled. WT LINC01123 combined with transfection of miR-4766-5p greatly decreased the luciferase activity in A549 and Calu-3 cells. Additionally, combined transfection of MUT LINC01123 and miR-4766-5p had a negligible effect on the luciferase activity (Fig. 4B). These results suggest that LINC01123 binds to miR-4766-5p through the WT binding sites. The protein Ago2 is a key component in miRNA-mediated RISC. We further identified that the abundances of LINC01123 and miR-4766-5p were greatly increased by anti-Ago2 RIP. This suggests that LINC01123 was involved in miR-4766-5p-regulated RISC (Fig. 4C). RT-qPCR analysis showed that the miR-4766-5p abundance decreased in tumor specimens and A549 and Calu-3 cells, unlike in the controls (Fig. 4D,E). Moreover, a negative association between miR-4766-5p expression and LINC01123 expression was uncovered in the tumor samples (Fig. 4F). These outcomes show that miR-4766-5p is a downstream target of LINC01123.

LINC01123 depletion promoted miR-4766-5p expression to repress lung adenocarcinoma cell activities

Considering the binding of LINC01123 to miR-4766-5p, we conducted rescue experiments to ascertain whether LINC01123 functions partially through

moderation of miR-4766-5p. The si-lnc-transfected cells exhibited considerable upregulation of miR-4766-5p. On the other hand, miR-4766-5p inhibitor-transfected cells had reduced levels of miR-4766-5p. Relative to si-lnc transfection only, miR-4766-5p expression substantially declined in cells transfected with both si-lnc plus inhibitor (Fig. 5A). Functionally, the proliferative and migration capacities of A549 and Calu-3 cells were noticeably increased by miR-4766-5p inhibitor (Fig. 5B,C). Moreover, the si-lnc-induced inhibition of proliferation and migration was partially reversed by the presence of miR-4766-5p inhibitor (Fig. 5B,C). Furthermore, miR-4766-5p inhibitor lowered Bax and enhanced Bcl-2 protein levels in A549 and Calu-3 cells. The enhanced Bax and reduced Bcl-2 protein levels engendered by LINC01123 depletion were partially reversed in the absence of miR-4766-5p (Fig. 5D). Our findings demonstrate that LINC01123 depletion represses lung adenocarcinoma cell activities by promoting miR-4766-5p expression.

MiR-4766-5p binds to the PYCR1 3'-UTR

MiRNAs are well-recognized for modulating the expressions of downstream functional genes. A publicly available tool, TargetScan, was utilized for target prediction. As depicted in Figure 6A, miR-4766-5p contained a potential binding site for the PYCR1 3'-

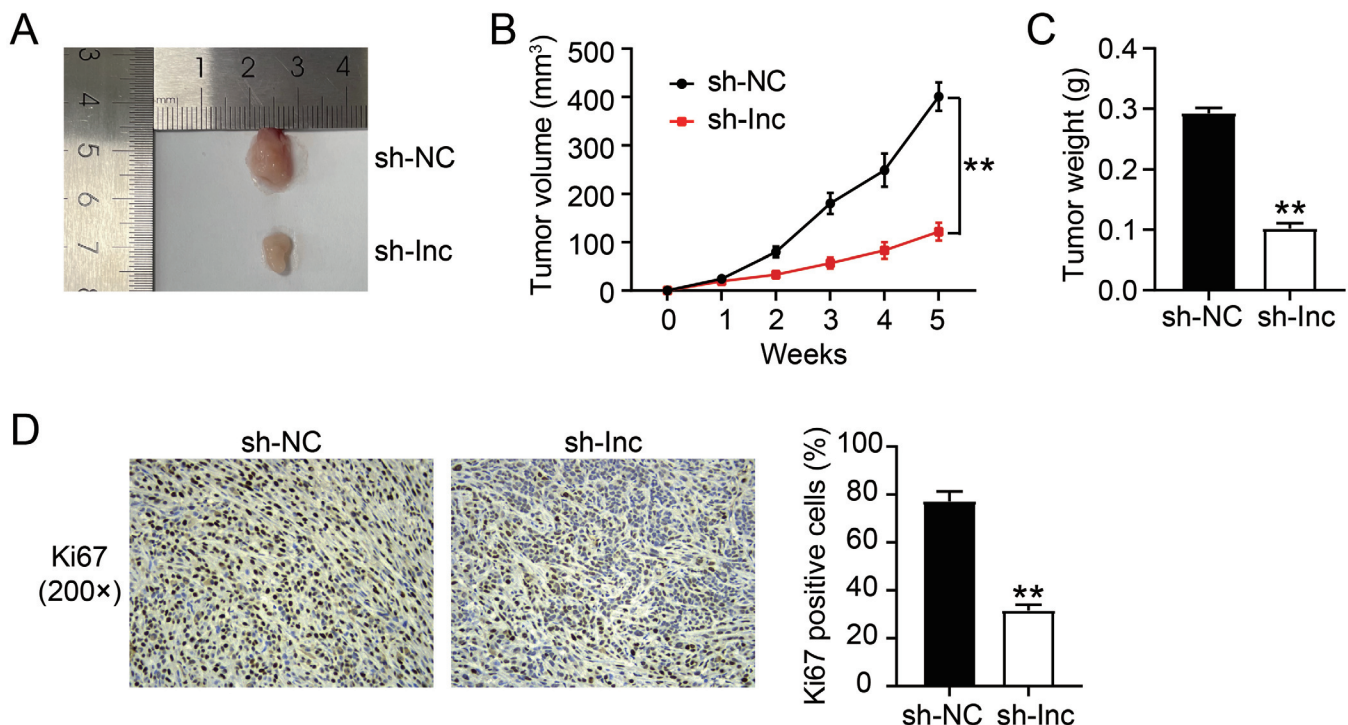


Fig. 3. LINC01123 knockdown inhibited tumor growth in vivo. Animal models were generated by injecting A549 cells (2×10^6 cells/mouse, with the infection of sh-lnc or sh-NC) into nude mice to ascertain the influence of LINC01123 knockdown on tumor growth. **A.** Representative images of tumor in sh-NC and sh-lnc groups. **B.** Tumor volume was weekly measured. **C.** Tumor weight was calculated after tumor tissues excised after 5 weeks. **D.** IHC staining for Ki67 was performed to assess the change of tumor growth. ****** $P < 0.01$ versus sh-NC.

LINC01123 drives lung adenocarcinoma progression

UTR. To confirm the predicted binding site, the WT and MUT constructs of the PYCR1 3'-UTR were assembled. Co-transfection of WT PYCR1 and miR-4766-5p mimic into A549 and Calu-3 cells greatly decreased the luciferase activity (Fig. 6B), thus indicating binding of miR-4766-5p to the PYCR1 3'-UTR. By expression analysis, the abundance of PYCR1 was found to be

increased in the Calu-3 and A549 cells, unlike in BEAS-2B cells (Fig. 6C). Additionally, PYCR1 expression was higher in the tumor specimens than in normal samples (Fig. 6D). Moreover, the miR-4766-5p expression in tumor samples was shown to have a negative association with PYCR1 expression (Fig. 6E). These findings indicate that PYCR1 is targeted by miR-4766-5p.

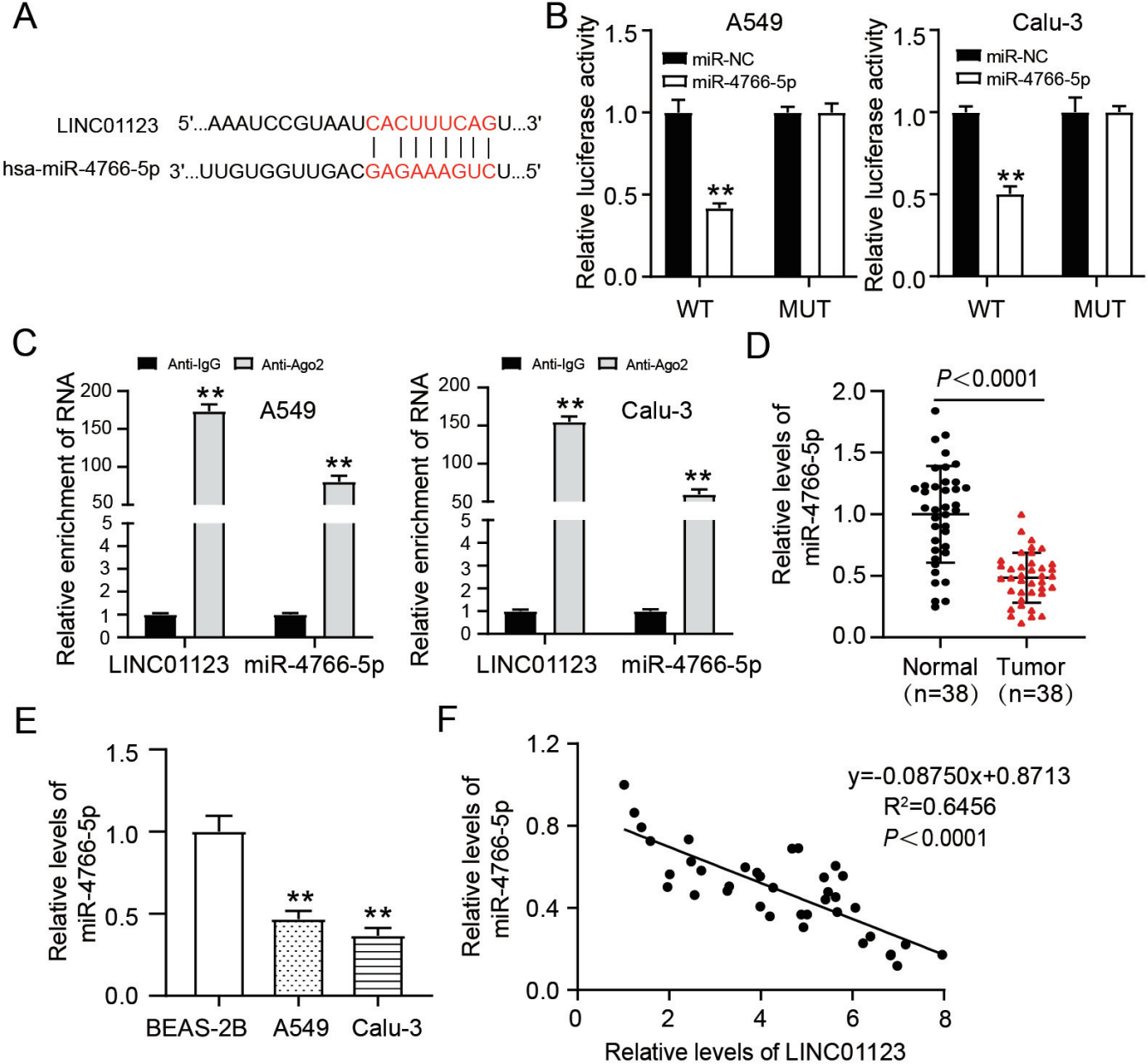


Fig. 4. LINC01123 bound to miR-4766-5p. A. Predicted binding sites of LINC01123 and miR-4766-5p, obtained using starBase (https://starbase.sysu.edu.cn/). B. Dual-luciferase reporter experiment was applied for the verification of the miR-4766-5p/ LINC01123 binding sites, ** $P < 0.01$ versus miR-NC. C. RIP experiment was applied for the verification of the binding between LINC01123 and miR-4766-5p, ** $P < 0.01$ versus Anti-IgG. D. MiR-4766-5p expression in non-cancer cell line (BEAS-2B) and lung adenocarcinoma cell lines (A549 and Calu-3). E. MiR-4766-5p expression in tumor and normal samples, ** $P < 0.01$ versus BEAS-2B. F. The correlation between miR-4766-5p expression and LINC01123 expression in tumor samples ($P < 0.0001$).

LINC01123 drives lung adenocarcinoma progression

The anticancer effects of PYCR1 downregulation were attenuated by the absence of miR-4766-5p

Given that miR-4766-5p binds directly to PYCR1,

we explored whether miR-4766-5p blocked the functional effects of PYCR1 in lung adenocarcinoma cells. The PYCR1 protein level was greatly reduced in si-PYCR1-transfected cells but was increased in

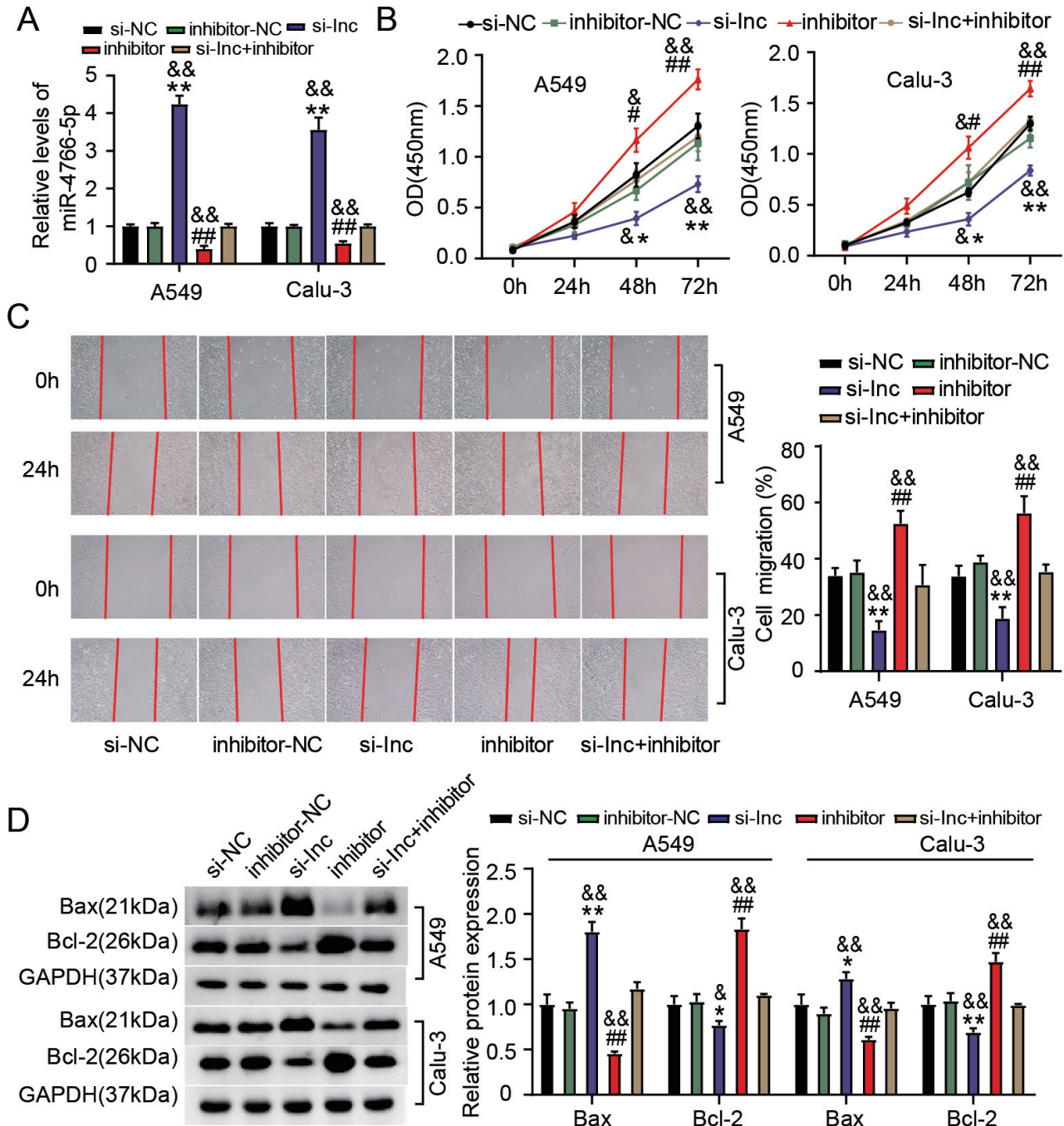


Fig. 5. LINC01123 depletion promoted miR-4766-5p expression to repress lung adenocarcinoma cell activities. A549 and Calu-3 cells were introduced with si-Lnc, si-NC, inhibitor, inhibitor-NC or si-Lnc+inhibitor. **A.** MiR-4766-5p expression levels in these transfected cells were checked by RT-qPCR. **B.** Cell proliferation in these transfected cells was assessed by CCK-8 analysis. **C.** Cell migration in these transfected cells was assessed by wound-healing study. **D.** The protein levels of Bax and Bcl-2 in these cells were ascertained by western blotting. * $P < 0.05$ and ** $P < 0.01$ versus si-NC; # $P < 0.05$ and ## $P < 0.01$ versus inhibitor-NC; & $P < 0.05$ and && $P < 0.01$ versus si-Lnc+inhibitor.

LINC01123 drives lung adenocarcinoma progression

inhibitor-transfected cells. Compared to cells transfected with only si-PYCR1, PYCR1 expression was substantially recovered by the transfection of si-PYCR1 + inhibitor into A549 and Calu-3 cells (Fig. 7A). Functionally, PYCR1 downregulation reduced the proliferative and migratory capabilities of A549 and Calu-3 cells. Additionally, compared to transfection of si-PYCR1 only, the cell proliferation and migration recovered considerably following co-transfection of si-PYCR1 + inhibitor (Fig. 7B,C). Additionally, PYCR1 downregulation increased Bax expression and reduced Bcl-2 expression. The elevation of Bax and reduction of Bcl-2 levels, brought about by PYCR1 downregulation, were reversed by miR-4766-5p inhibition (Fig. 7D). These data indicate that miR-4766-5p binds to PYCR1, thus affecting the function of PYCR1 in lung adenocarcinoma.

Discussion

There is growing interest in the function and mechanism of lncRNAs in diverse types of carcinogenesis (Lv et al., 2020). Dysregulated lncRNAs have been established as diagnostic markers, prognostic biomarkers, and treatment-responsive predictors in lung cancer (Ricciuti et al., 2016; Peng et al., 2017). Here, we

demonstrated the carcinogenic role of LINC01123 in lung adenocarcinoma, as its depletion resulted in repressive effects on the development of lung adenocarcinoma cells and in vivo tumorigenicity. We further identified the binding relationship between miR-4766-5p and LINC01123 or PYCR1. Moreover, their interactions in lung adenocarcinoma cell development were further unveiled through rescue experiments. Our study explored a new regulatory network targeted by LINC01123.

Compelling evidence shows that LINC01123 functions as an oncogenic driver in the tumorigenesis of numerous cancers. Xiao et al. have documented the elevated expression of LINC01123 in hepatocellular carcinoma (Xiao et al., 2020b). They also showed that the absence of LINC01123 restrained the growth and invasive ability of hepatocellular carcinoma cells and impeded solid tumor growth in the animal models (Xiao et al., 2020b). Ye et al. reported that LINC01123 is highly expressed in colon cancer cell lines (Ye et al., 2020). Furthermore, LINC01123 ectopic expression promoted colon cancer cell proliferation and motility, angiogenesis, and chemoresistance (Ye et al., 2020). Regarding the role of LINC01123 in lung cancer, its elevated expression has been demonstrated to predict low survival (Hua et al., 2019). LINC01123 has also

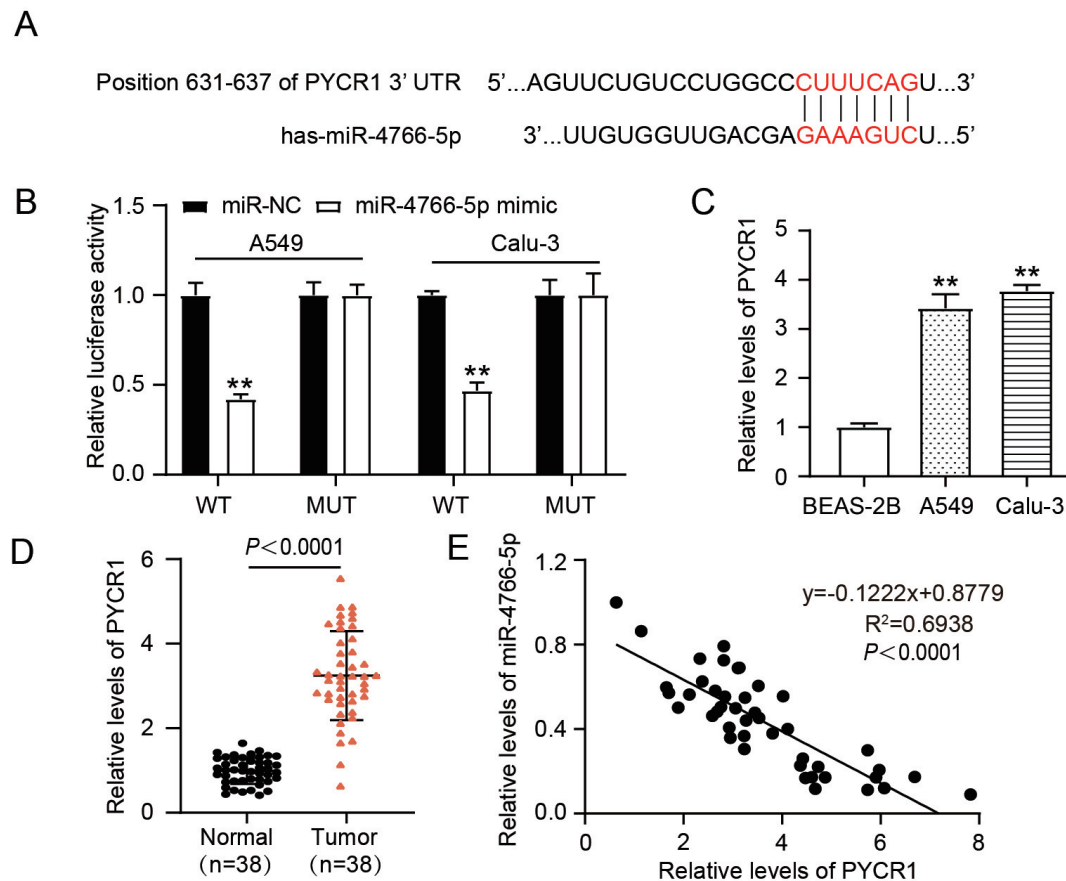


Fig. 6. MiR-4766-5p bound to PYCR1 3'UTR. **A.** The predicted binding site between miR-4766-5p and PYCR1 3'UTR was obtained from TargetScan (https://www.targetscan.org/vert_72/). **B.** MiR-4766-5p and PYCR1 3'UTR binding site confirmed via dual-luciferase reporter analysis, ** $P < 0.01$ versus miR-NC. **C.** PYCR1 mRNA expression in non-cancer cell line (BEAS-2B) and lung adenocarcinoma cell lines (A549 and Calu-3), ** $P < 0.01$ versus BEAS-2B. **D.** PYCR1 mRNA expression in tumor and normal samples. **E.** The association between miR-4766-5p and PYCR1 expressions in tumor samples ($P < 0.0001$).

LINC01123 drives lung adenocarcinoma progression

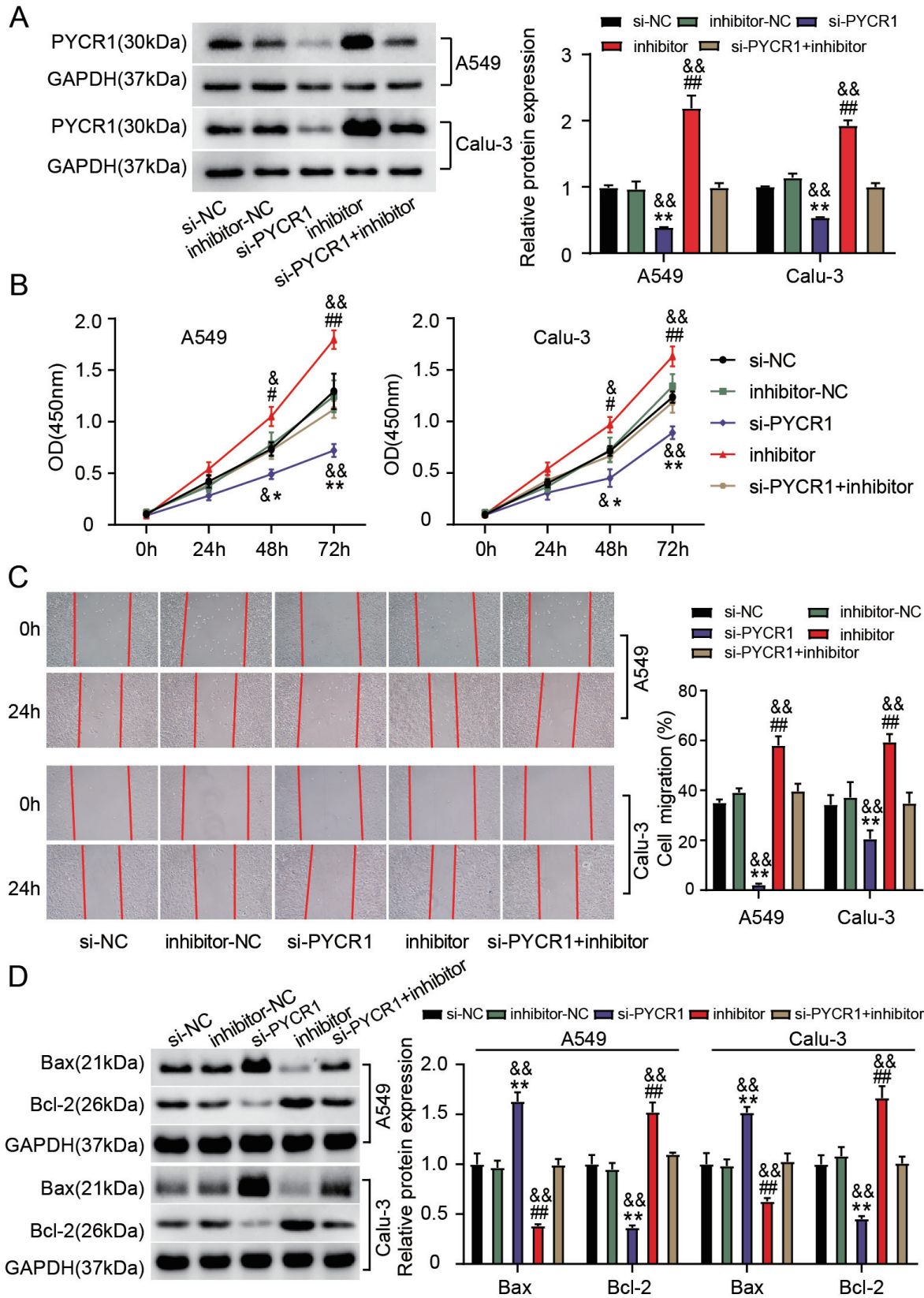


Fig. 7. The absence of miR-4766-5p attenuated the anti-cancer effects of PYCR1 downregulation. A549 and Calu-3 cells were introduced with si-PYCR1, si-NC, inhibitor, inhibitor-NC or si-PYCR1+inhibitor. **A.** PYCR1 protein expression in these transfected cells was checked via western blotting. **B.** Cell proliferation was assessed via CCK-8 analysis. **C.** Cell migration in these cells was assessed via wound-healing assay. **D.** The protein expressions of Bax and Bcl-2 among the transfected cells were ascertained through western blotting. * $P < 0.05$ and ** $P < 0.01$ versus si-NC; # $P < 0.05$ and ## $P < 0.01$ versus inhibitor-NC; & $P < 0.05$ and && $P < 0.01$ versus si-PYCR1+inhibitor.

LINC01123 drives lung adenocarcinoma progression

been reported to increase NSCLC cell proliferation and aerobic glycolysis, thereby promoting NSCLC development (Hua et al., 2019). In addition, LINC01123 was found to be transcriptionally activated by the ZEB1 transcriptional factor in lung adenocarcinoma; the elevated expression of LINC01123 was also reported to be responsible for cancer cell malignant functions, including survival, epithelial-mesenchymal transition (EMT), and proliferation (Zhang et al., 2020). In agreement with these studies, we confirmed the repressive influence of LINC01123 depletion on the migration and proliferation of lung adenocarcinoma cells as well as tumor growth in animal models. These consistent findings indicate that LINC01123 is an oncogenic driver in cancer initiation and development. Restriction of LINC01123 expression may be a key strategy in lung adenocarcinoma management.

Consistent with an earlier study, we observed a high abundance of LINC01123 in the cytoplasmic fractions of lung cancer cells (Hua et al., 2019). This suggests that LINC01123 may serve as a competing endogenous RNA (ceRNA) that modulates mRNA and decoys miRNA. Our study is the first to validate LINC01123/miR-4766-5p binding. MiR-4766-5p deficiency is thought to increase breast cancer growth, metastasis, and chemoresistance by upregulation of the oncogene sirtuin 1 (SIRT1) (Liang et al., 2018). Similarly, low expression of miR-4766-5p has also been reported in colorectal cancer (Zhan et al., 2020). The LINC00858-knockdown-induced reduction of cell proliferative, migratory, and invasive capacities was restored by increased miR-4766-5p levels (Zhan et al., 2020). MiR-4766-5p has been reported to exhibit similar anticancer properties in gastric cancer (Peng et al., 2020). In our work, we confirmed that a lack of miR-4766-5p increased lung adenocarcinoma cell proliferation and migration. LINC01123 sponged miR-4766-5p to block its anticancer effects in lung adenocarcinoma. This shows that the absence of miR-4766-5p reversed the effects of LINC01123 depletion. Alleviating the LINC01123-induced inhibition of miR-4766-5p may be a feasible strategy for lung adenocarcinoma therapy.

We also characterized the functional genes targeted by miR-4766-5p and discovered that LINC01123 shares a miR-4766-5p binding site with the PYCR1 3'-UTR. This implies that LINC01123 may compete with PYCR1 for the miR-4766-5p binding site. Previous studies have reported that PYCR1 is negatively regulated by miR-488, and ectopic expression of PYCR1 in lung cancer cells enhanced their proliferation while attenuating apoptosis (Cai et al., 2018; Wang et al., 2019a). PYCR1 is a predictor of poor prognosis and is expressed at high levels in lung adenocarcinoma (Gao et al., 2020). Knockdown of PYCR1 reduced the proliferative, migratory, and invasive abilities of lung adenocarcinoma cells by regulating the activity of JAK/STAT signaling (Gao et al., 2020). Moreover, PYCR1 overexpression has also been linked to aggressive cancer cell behaviors in other types of cancers, such as hepatocellular

carcinoma, bladder, and colorectal cancer (Yan et al., 2019; Zhuang et al., 2019; Du et al., 2021). Overall, these findings are evidence of its oncogenic property in cancer development. Our study confirmed the binding relationship between miR-4766-5p and PYCR1. Silencing PYCR1 restrained lung adenocarcinoma cell growth and migration. Additionally, a lack of miR-4766-5p enhanced the abundance of PYCR1, thus attenuating the anticancer effects of PYCR1 knockdown. Our data confirm the interaction between miR-4766-5p and PYCR1 in lung adenocarcinoma progression.

Our study elucidated the role of the LINC01123/miR-4766-5p/PYCR1 pathway in lung adenocarcinoma development. PYCR1 is an enzyme located in the inner mitochondrial membrane and affects metabolic stress responses (Kuo et al., 2020; Xiao et al., 2020a). In light of this, whether LINC01123 regulates metabolic stress in lung adenocarcinoma by mediating the miR-4766-5p/PYCR1 axis warrants investigation.

Conclusion

LINC01123 enhances lung adenocarcinoma cell growth and migration, thereby promoting tumorigenesis. It functions as an oncogenic driver in lung adenocarcinoma at least in part by modulating the miR-4766-5p/PYCR1 axis. Our findings indicate that the therapeutic application of targeting LINC01123 in lung adenocarcinoma has ample potential.

Acknowledgements. None.

Funding. Funding information is not available.

Conflicts of interest. The authors declare that they have no conflicts of interest.

Ethics approval. This research has been approved by the Ethics Committee of the First Affiliated Hospital of Chengdu Medical College (Chengdu, China). The processing of clinical samples had been in strict compliance with the ethical standards of the Declaration of Helsinki. All patients provided their written informed consent.

The procedures executed in the animal study were approved by the First Affiliated Hospital of Chengdu Medical College. All animal experiments comply with the ARRIVE guidelines.

Consent to participate. All patients signed a written informed consent.

Consent for publication. Not applicable.

Availability of data and material. All data generated or analyzed during this study are included in this article.

Authors' contributions. HW and DSH performed the experiments and data analysis. HW designed and devised the study. DSH obtained the data. HW and DSH processed and interpreted the data. This manuscript has been read and approved by all authors

References

- Cai F., Miao Y., Liu C., Wu T., Shen S., Su X. and Shi Y. (2018). Pyrroline-5-carboxylate reductase 1 promotes proliferation and inhibits apoptosis in non-small cell lung cancer. *Oncol. Lett.* 15, 731-740.
- Du S., Sui Y., Ren W., Zhou J. and Du C. (2021). PYCR1 promotes

LINC01123 drives lung adenocarcinoma progression

- bladder cancer by affecting the Akt/Wnt/ β -catenin signaling. *J. Bioenerg. Biomembr.* 53, 247-258.
- Gao Y., Luo L., Xie Y., Zhao Y., Yao J. and Liu X. (2020). PYCR1 knockdown inhibits the proliferation, migration, and invasion by affecting JAK/STAT signaling pathway in lung adenocarcinoma. *Mol. Carcinog.* 59, 503-511.
- Gomez-Verjan J.C., Vazquez-Martinez E.R., Rivero-Segura N.A. and Medina-Campos R.H. (2018). The RNA world of human ageing. *Hum. Genet.* 137, 865-879.
- Gridelli C., Rossi A., Carbone D.P., Guarize J., Karachaliou N., Mok T., Petrella F., Spaggiari L. and Rosell R. (2015). Non-small-cell lung cancer. *Nat. Rev. Dis. Primers* 1, 15009.
- Hua Q., Jin M., Mi B., Xu F., Li T., Zhao L., Liu J. and Huang G. (2019). LINC01123, a c-Myc-activated long non-coding RNA, promotes proliferation and aerobic glycolysis of non-small cell lung cancer through miR-199a-5p/c-Myc axis. *J. Hematol. Oncol.* 12, 91.
- Kuo C.L., Chou H.Y., Chiu Y.C., Cheng A.N., Fan C.C., Chang Y.N., Chen C.H., Jiang S.S., Chen N.J. and Lee A.Y. (2020). Mitochondrial oxidative stress by Lon-PYCR1 maintains an immunosuppressive tumor microenvironment that promotes cancer progression and metastasis. *Cancer Lett.* 474, 138-150.
- Lee S. and Vasudevan S. (2013). Post-transcriptional stimulation of gene expression by microRNAs. *Adv. Exp. Med. Biol.* 768, 97-126.
- Lee K.H., Hwang H.J. and Cho J.Y. (2020). Long non-coding RNA associated with Cholesterol homeostasis and its involvement in metabolic diseases. *Int. J. Mol. Sci.* 21, 8337.
- Liang Y., Song X., Li Y., Sang Y., Zhang N., Zhang H., Liu Y., Duan Y., Chen B., Guo R., Zhao W., Wang L. and Yang Q. (2018). A novel long non-coding RNA-PRLB acts as a tumor promoter through regulating miR-4766-5p/SIRT1 axis in breast cancer. *Cell Death Dis.* 9, 563.
- Lu T., Yang X., Huang Y., Zhao M., Li M., Ma K., Yin J., Zhan C. and Wang Q. (2019). Trends in the incidence, treatment, and survival of patients with lung cancer in the last four decades. *Cancer Manag. Res.* 11, 943-953.
- Lv Y., Wang Z., Zhao K., Zhang G., Huang S. and Zhao Y. (2020). Role of noncoding RNAs in cholangiocarcinoma (Review). *Int. J. Oncol.* 57, 7-20.
- Martens-Uzunova E.S., Böttcher R., Croce C.M., Jenster G., Visakorpi T. and Calin G.A. (2014). Long noncoding RNA in prostate, bladder, and kidney cancer. *Eur. Urol.* 65, 1140-1151.
- Peng F., Wang R., Zhang Y., Zhao Z., Zhou W., Chang Z., Liang H., Zhao W., Qi L., Guo Z. and Gu Y. (2017). Differential expression analysis at the individual level reveals a lncRNA prognostic signature for lung adenocarcinoma. *Mol. Cancer* 16, 98.
- Peng L., Chen Z., Wang G., Tian S., Kong S., Xu T., An X. and Chen Y. (2020). Long noncoding RNA LBX2-AS1-modulated miR-4766-5p regulates gastric cancer development through targeting CXCL5. *Cancer Cell. Int.* 20, 497.
- Ricciuti B., Mencaroni C., Pagliarlunga L., Paciullo F., Crinò L., Chiari R. and Metro G. (2016). Long noncoding RNAs: New insights into non-small cell lung cancer biology, diagnosis and therapy. *Med. Oncol.* 33, 18.
- Shi T., Morishita A., Kobara H. and Masaki T. (2021). The role of long non-coding RNA and microRNA networks in hepatocellular carcinoma and its tumor microenvironment. *Int. J. Mol. Sci.* 22, 10630.
- Siegel R.L., Miller K.D. and Jemal A. (2017). Cancer statistics, 2017. *CA Cancer J. Clin.* 67, 7-30.
- Stella G.M., Luisetti M., Pozzi E. and Comoglio P.M. (2013). Oncogenes in non-small-cell lung cancer: Emerging connections and novel therapeutic dynamics. *Lancet Respir. Med.* 1, 251-261.
- Sung H., Ferlay J., Siegel R.L., Laversanne M., Soerjomataram I., Jemal A. and Bray F. (2021). Global cancer statistics 2020: GLOBOCAN estimates of incidence and mortality worldwide for 36 cancers in 185 countries. *CA Cancer J. Clin.* 71, 209-249.
- Tutar Y., Özgür A., Tutar E., Tutar L., Pulliero A. and Izzotti A. (2016). Regulation of oncogenic genes by microRNAs and pseudogenes in human lung cancer. *Biomed. Pharmacother.* 83, 1182-1190.
- Wang D., Wang L., Zhang Y., Yan Z., Liu L. and Chen G. (2019a). PYCR1 promotes the progression of non-small-cell lung cancer under the negative regulation of miR-488. *Biomed. Pharmacother.* 111, 588-595.
- Wang M., Mao C., Ouyang L., Liu Y., Lai W., Liu N., Shi Y., Chen L., Xiao D., Yu F., Wang X., Zhou H., Cao Y., Liu S., Yan Q., Tao Y. and Zhang B. (2019b). Long noncoding RNA LINC00336 inhibits ferroptosis in lung cancer by functioning as a competing endogenous RNA. *Cell Death Differ.* 26, 2329-2343.
- Wei Y., Wang Y., Zang A., Wang Z., Fang G. and Hong D. (2019). MiR-4766-5p inhibits the development and progression of gastric cancer by targeting NKAP. *Onco Targets Ther.* 12, 8525-8536.
- Xiao S., Li S., Yuan Z. and Zhou L. (2020a). Pyrroline-5-carboxylate reductase 1 (PYCR1) upregulation contributes to gastric cancer progression and indicates poor survival outcome. *Ann. Transl. Med.* 8, 937.
- Xiao Z., Liu Y., Zhao J., Li L., Hu L., Lu Q., Zeng Z., Liu X., Huang D., Yang W. and Xu Q. (2020b). Long noncoding RNA LINC01123 promotes the proliferation and invasion of hepatocellular carcinoma cells by modulating the miR-34a-5p/TUFT1 axis. *Int. J. Biol. Sci.* 16, 2296-2305.
- Yan K., Xu X., Wu T., Li J., Cao G., Li Y. and Ji Z. (2019). Knockdown of PYCR1 inhibits proliferation, drug resistance and EMT in colorectal cancer cells by regulating STAT3-mediated p38 MAPK and NF- κ B signalling pathway. *Biochem. Biophys. Res. Commun.* 520, 486-491.
- Ye S., Sun B., Wu W., Yu C., Tian T., Lian Z., Liang Q. and Zhou Y. (2020). LINC01123 facilitates proliferation, invasion and chemo-resistance of colon cancer cells. *Biosci. Rep.* 40, BSR20194062.
- Zamaraev A.V., Volik P.I., Sukhikh G.T., Kopeina G.S. and Zhivotovsky B. (2021). Long non-coding RNAs: A view to kill ovarian cancer. *Biochim. Biophys. Acta Rev. Cancer* 1876, 188584.
- Zhan W., Liao X., Chen Z., Li L., Tian T., Yu L. and Li R. (2020). LINC00858 promotes colorectal cancer by sponging miR-4766-5p to regulate PAK2. *Cell. Biol. Toxicol.* 36, 333-347.
- Zhang M., Han Y., Zheng Y., Zhang Y., Zhao X., Gao Z. and Liu X. (2020). ZEB1-activated LINC01123 accelerates the malignancy in lung adenocarcinoma through NOTCH signaling pathway. *Cell Death Dis.* 11, 981.
- Zhuang J., Song Y., Ye Y., He S., Ma X., Zhang M., Ni J., Wang J. and Xia W. (2019). PYCR1 interference inhibits cell growth and survival via c-Jun N-terminal kinase/insulin receptor substrate 1 (JNK/IRS1) pathway in hepatocellular cancer. *J. Transl. Med.* 17, 343.